2024 IEEE/RSJ International Conference on Intelligent Robots and Systems (IROS)
October 14-18, 2024. Abu Dhabi, UAE

Bistable valve for electronics-free soft robots

Kan Longxin, Lam Jia Qing Joshua, Qin Zhihang, Li Keyi, Tang Zhiqiang, and Cecilia Laschi*, *Fellow, IEEE*

Abstract— **Recently, there has been a notable shift towards electronics-free designs, which offer promising integration possibilities with soft robots, reducing reliance on traditional electronics. Despite numerous demonstrations showcasing logical control, contact sensors, and gait control, the conventional quake valve-based design is gradually struggling to meet the demands of electronics-free soft robots with increasingly complex functionalities. Integrating multiple tubes, channels, and valves has led to larger and bulkier overall systems. In this study, we introduce a simple yet powerful electronics-free pneumatic valve that excels in various aspects: it allows for flexible function configurations (operating individually, in pairs, or in larger groups), offers high-frequency synchronous reverse outputs, stores valve status, and ensures efficient maintenance. We believe that this work lays the groundwork for developing straightforward yet highly effective fully autonomous soft robots.**

I. Introduction

Over the past decade, we have witnessed rapid development in the field of soft robotics (1,2). A large number of researchers worldwide aim to build fully autonomous soft robotic systems by introducing various actuation methods (3-8) and control strategies (9-11).

However, building fully autonomous soft robotic systems still remains a challenge due to the reliance on rigid bulk electronics and control components (12,13), which significantly compromise the flexibility of the entire soft system. Despite considerable global efforts, progress in this regard has been limited. Recently, emerging designs of electronics-free fluidic circuits have shown the potential to be seamlessly integrated into soft robots and reduce the dependence on rigid electronics (14-16), garnering increased attention from researchers.

The development of electronics-free valves stands as a paramount priority in constructing electronics-free robotic systems (17-19). These valves play a crucial role in transforming constant air pressure supply into periodic oscillatory air outputs (14,20,21,22). Thanks to concerted global efforts in this domain, numerous invaluable electronics-free valve designs have emerged, such as the quake valve (15,16), buckling-sheet valve (20), tube-balloon logic valve (23), and even 3D-printed soft valves (24,25).

Although a plethora of valuable valves have been reported, their basic principles remain similar, with the key lying in the blocking and recovery of tubes or channels. This process is typically governed by the inflation and deflation of chambers, which are used to govern the airflow in the valves. Hence, inflate channels and deflate channels need to be connected to the chambers and opened and closed alternately. While the inherent functional diversity of valves may seem relatively modest, they have served as the foundation for various demonstrations, including logical control (16,26,27), contact sensors (15), the realization of various walking gaits for soft-legged quadrupeds (21), and even the development of strategies for digital and analog control using electronics-free soft valves (28).

However, most electronics-free pneumatic valves can only control airflow in a single channel, necessitating at least two valves to manage airflow in both the inflate and deflate channels. A typical strategy involves connecting three valves (e.g., valves A, B, and C, each functioning as a "NOT" gate) end-to-end (15,23,24). Valve A controls the inflation and deflation of valve B, valve B controls the inflation and deflation of valve C, and valve C controls the inflation and deflation of valve A. While this configuration is useful, employing too many valves increases the complexity and weight of the entire system, posing a challenge to the construction of untethered soft robots. Additionally, most reported electronics-free soft oscillators consist of three valves (where all three valves function as a "NOT" gate), exhibit poor scalability in terms of the number of valves. They require an odd number (no fewer than 3) of "NOT" gate valves to construct a closed ring oscillator loop, which is not suitable for specific scenarios that require only one or an even number of valves.

Another approach involves integrating multiple tubes into a single valve (29), thereby enabling one valve to control the airflow of several tubes. However, integrating too many tubes can introduce new challenges. This is because most valves rely on the elasticity of materials to return to their initial state when deflated. Integrating more tubes increases the resistance during recovery, making switching more difficult, reducing the number of cycles, and potentially causing air leakage. Moreover, integrating more tubes requires additional space, resulting in a larger and heavier valve.

In addition, there are also some disadvantages in the currently reported valves. For instance, the state of valves cannot be maintained after the air supply is shut down because the chambers used to control the valve state will return to their original state when deflating. Moreover, it is difficult to maintain and replace faulty parts due to the closed structural design.

Therefore, there is an urgent need to propose a new, simplified valve design for the control of autonomous soft robots. To bridge this gap, we design and fabricate a simple yet powerful soft valve that excels in terms of scalability, synchronous reverse outputs, valve status storage, and efficient maintenance. Our soft valve can function individually, in pairs, in triples, or in any other configuration.

All authors are with Department of Mechanical Engineering, National University of Singapore, Singapore, Singapore (e-mail: mpeclc@nus.edu.sg).

With our design, we can effortlessly convert a constant air supply into periodic oscillation outputs, enabling a soft robot to produce rhythmic movements resembling Central Pattern Generator (CPG) mechanisms, with just a single constant air supply.

II. Design of Bistable Valve

Figure 1 illustrates the design of a bistable valve, featuring a rhombus structure comprising four soft silicone tubes. This design incorporates two kink points and two non-kink points simultaneously, enabling the automatic separation of the inflation and deflation channels. Consequently, four tubes (t1-t4) were integrated into a compact structure (as depicted in Figure 1a), with 4 joints for switching the 4-tube rhombus. Additionally, we observed that this structure tends to maintain two states without external interference. And we define them as state 1 and state 2.

In state 1, tube 1 (t1) and tube 3 (t3) are kinked, with the air source and actuator connected to the atmosphere via tube 2 (t2) and tube 4 (t4) respectively, resulting in actuator deflation. Conversely, in state 2, tubes 2 (t2) and 4 (t4) remain kinked, while the air source connects directly to the actuator through tube 1, leading to actuator inflation.

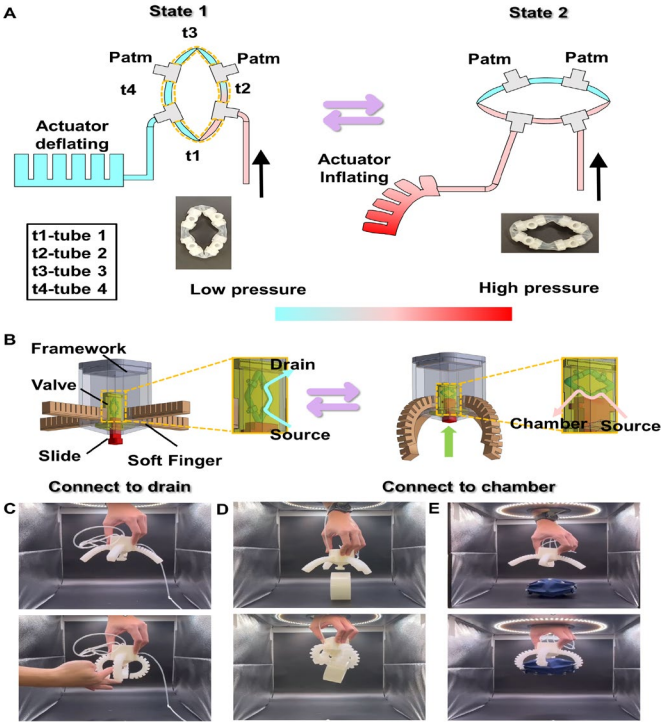

Figure 1. Design and operating principles for bistable valves. A) our proposed bistable valve consists of four soft tubes (t1, t2, t3, t4). Tube 1 and tube 3 kinked at state 1 while tube 2 and tube 4 kinked at state 2.B) Diagram of soft gripper shows the operating mechanism of integrated valve as a contact sensor. Soft gripper with integrated contact sensor will grasp C) Human finger. D) Tape, and. E) Soft pneumatic artificial muscle.

To demonstrate the manual switching between state 1 and state 2, we designed a soft gripper incorporating the bistable valve as a contact sensor, which helps control the air flow in the whole system. As depicted in Figure 1B, the gripper comprises a framework, four soft fingers, the bistable valve, and a slide. Upon release, the air source connects to the atmosphere via tube 2 (t2), rendering the fingers inactive. However, when the slide makes contact with an object when we manually applied a vertical force on the gripper framework, the valve compresses and switches its state due to the force applied in the vertical direction, directing the air source to the soft fingers via tube 1 (t1). This increases the pressure in the soft fingers, allowing them to grasp the target.

Figures 1C-E demonstrate the efficient grasping capabilities of the soft gripper on human fingers, tape, and soft pneumatic artificial muscle.

III. Finite Element Analysis of the Bistable Valve

The valve with rhombus structure exhibits two stable states when compressed in both horizontal and vertical directions. When it undergoes compression in a specific direction, the tubes perpendicular to this direction are released, while the tubes parallel to this direction bend and form a kinked shape. Throughout the structural deformation process, a quarter of the entire structure consistently maintains a plane-symmetrical deformation pattern.

To elucidate the bistable nature of our proposed valve, we utilized Finite Element Method (FEM) to conduct the simulation. Figure 2A and 2B illustrates how we simplify the structure to be simulated. The structure generated in the simulation is only a quarter of the overall structure at planar cross-sectional view of the rhombus structure. In this simulation, our focus was on the strain energy change of the rhombus-shaped structure, and we analyzed the deformation of this structure under quasi-static conditions, utilizing the ABAQUS 2020 software on the NUS HPC platform.

As the assembled flexible tubes of the rhombus structure were already in a buckled state, it is necessary to preset the specific stress and strain distribution on the structure to be simulated. To get the specific stress and strain distribution for presetting, the simulation should be completed in two separate jobs.

The first job is to achieve the specific stress and strain distribution for presetting by deforming a quarter of undeformed valve that contains both rigid block and flexible tubes to a desired shape like a quarter of rhombus. Then, we save the deformed structure and strain/stress distribution into the odb database for the next job. The second job is to utilize the deformed structure obtained in the first job, the specific stress and strain distribution for presetting, and the plane-symmetrical boundary conditions to generate a complete simulation of planar rhombus structure for the bistable behavior analysis.

Figure 2D illustrates the strain of planar rhombus structure under the compression in alternating horizontal and vertical directions. The grey part in Figure 2D is the rigid blocks of the rhombus structure. They were set as rigid bodies in the simulation. Hence, there is no strain on these blocks. Figure 2C illustrates the strain energy change of planar rhombus structure during the multiple compression process. When planar rhombus structure is compressed to one state in which two tubes are kinked while the other two are released, the overall strain energy approaches its minimum. The presence of multiple energy valleys resulting from the back-and-forth compression in both the x and y-axes serves as compelling evidence of its bistable nature.

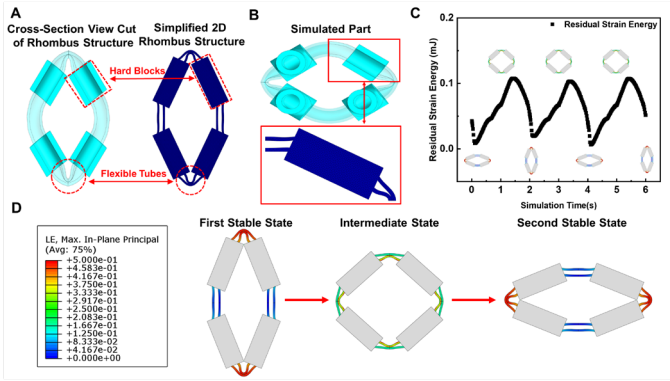

Figure 2. Finite Element Method Analysis of our proposed bistable valve. A) Schematic diagram of the simplified planar rhombus structure. B) Schematic diagram of the simulated part in the simulation. C) Strain energy change of the bistable structure. D) Strain Distributions of the bistable structure under different states.

IV. Design of the Pneumatically Operated Bistable Valve.

Our proposed bistable valve can be operated both manually and pneumatically. Although both methods utilize external force to compress the bistable valve, there are significant differences between the two strategies, as shown in Figure 3A. In manual switching, the external force and the air pressure in tubes (t1-t4) are independent. The variation of air pressure inside the tubes has no influence on the force applied to them. Therefore, a smooth switch can be achieved without encountering significant resistance.

However, the dynamics are significantly different in the pneumatically activated switch. As depicted in Figure 3B, we utilize two pairs of orthogonally placed small chambers with bistable membranes to assist in compressing the soft valve. One set of paired chambers (C1 and C3) is connected to the nodes of the tube and then linked to tube 5 (t5). Similarly, chambers C2 and C4 can be connected to tube 6 (t6) using the same approach. This allows us to control the inflation and deflation of the two pairs of chambers using pneumatic strategies. And the compressive force is generated by the inflation of soft chambers. Consequently, the compressive forces vary with changes in air pressure throughout the system. For instance, in state 1, the air source connects to chambers 1 and 3 via tube 2, prompting chambers 2 and 4 to commence inflating and applying a vertical force to the bistable valve. The valve begins transitioning to state 2. However, due to the slow switching speed, all tubes become unblocked in the middle state, causing compressed air to flow through the entire system and even leak directly from the drain. This results in a decrease in pressure within the channels and chambers, impeding the valve switch and leading to air leakage.

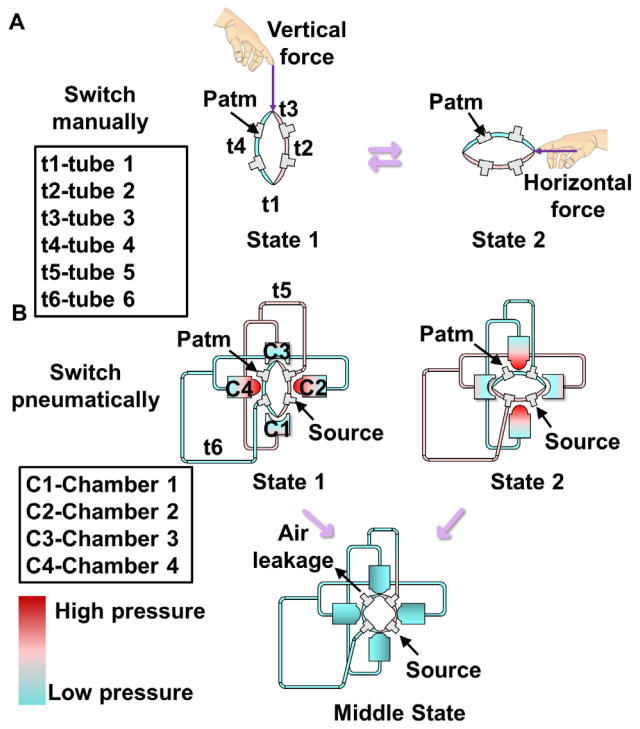

Figure 3. Manual and pneumatic switching of our proposed valve. A) The bistable valve can switch between state 1 and state 2 manually by applying vertical and horizontal forces. B) Air leakage in the middle state.

Therefore, the key point for the pneumatic strategy is to avoid the intermediate state and maintain the air pressure within the inflation channel at a sufficiently high level to facilitate valve switching.

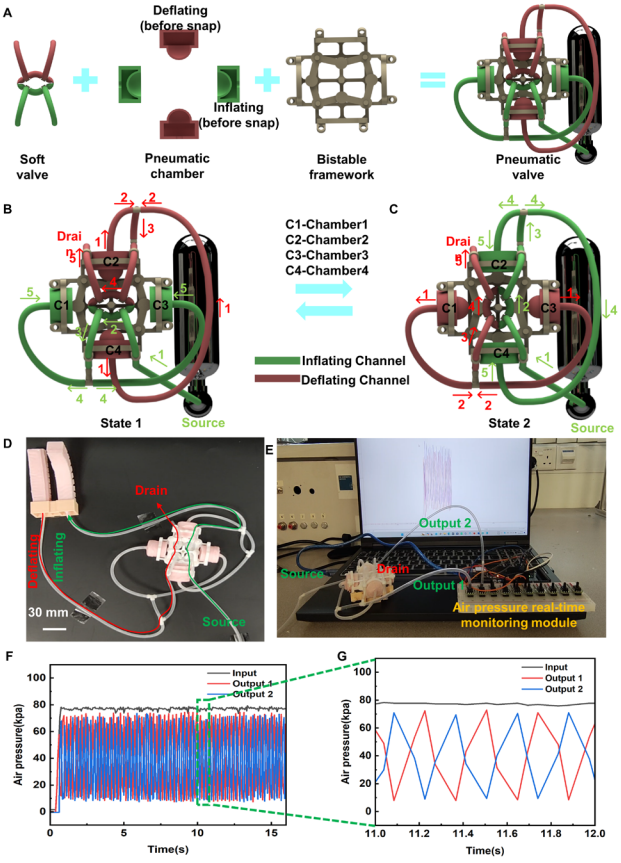

Figure 4. Design and pneumatic operating principles for single bistable valve. A) A rhombus structure consisting of four rigid joints and four soft silicone tube was proposed, which has two kink points and two non-kink points at the same time; owning to this structure, the inflation channel and deflation channel are automatically separated. B-C) We add four orthogonally placed small chambers with bistable membranes, which connect to other pressed air from other units and inflate or deflate corresponding to control the state of bistable rhombus tubes. D) The source and drain are diagonally positioned, with the chamber directly connected to the source for inflation, while connected to the drain for deflation. The unit's dimensions are 70mm x 70mm x 30mm. E) The real-time monitoring settings of output 1. F-G) The air pressure varies between 10KPa and 75KPa with a frequency of about 5HZ when an 80KPa air pressure is applied, and a frequency of approximately 12 Hz was detected when 150 KPa of air pressure was applied.

Figure 4 illustrates the mechanism of our proposed single pneumatically switch valve with a switching speed enhancement framework (as depicted in the Figure 4A). We define the whole system as a unit. We designate two distinct states as state 1 and state 2 (as depicted in the Figure 4B and 4C). When the chamber is directly connected to the source, it inflates (highlighted in green), whereas it will deflate (highlighted in red) when directly connected to the drain. Additionally, we have the ability to switch the state of chambers by altering the states of the valves, a feat achieved by introducing four orthogonally placed small chambers with bistable membranes. We refer to the entire structure as a single unit. These chambers are interconnected with other units, and each unit utilizes a pneumatic signal as input to alter its state.

Furthermore, the inflation and deflation channels are automatically separated at the tube's kink point. We employ the colors green and red to distinguish between the inflation channel and the deflation channel, respectively, for the sake of clarity.

In state 1 (depicted in Figure 4B), the inflation channel (green) connects the source to Chamber1(C1) and Chamber3(C3), while the deflation channel (red) connects the drain to Chamber2(C2) and Chamber4(C4). Consequently, C1 and C3 inflates, and C2, C4 deflates in state 1. Which helps the middle valve switch to state 2. Conversely, in state 2 (depicted in Figure 4C), the situation is reversed. The old channels are blocked, and new channels are formed. The new inflation channel (green) connects the source to Chamber2(C2) and Chamber4(C4), while the deflation channel (red) connects the drain to Chamber1(C1) and Chamber3(C3). This results in C2, C4 inflating and C1, C3 deflating in state 2.

Figures 4F and 4G depict the variations in air pressure in Chamber1(C1) and Chamber3(C3) (output 1) and Chamber2(C2) and Chamber4(C4) (output 2) based on real-time air pressure monitoring (as shown in Figures 5D and 5E). With this design, we can easily generate a pair of synchronous reverse outputs with a single constant input (slight air pressure decrease detected because we used a pump that inflates first and then exhausts). The air pressure varies between 10 KPa and 75 KPa with a frequency of about 5 Hz when an 80 KPa air pressure is applied, and a frequency of approximately 12 Hz was detected when 150 KPa of air pressure was applied. which is much faster than most reported designs (15,16,20,24,25).

V. Ring Oscillators

Our proposed units are designed to operate both independently and as integrated components within a ring oscillator. Typically, a ring oscillator consists of three units, all functioning as "NOT" gates. They inflate and deflate alternately to generate oscillation.

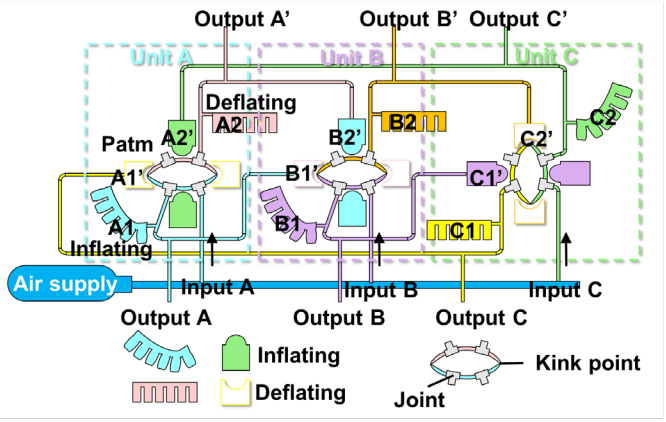

Figure 5. Three units are connected end-to-end to form a soft ring oscillator, enabling sequential inflation and deflation of different actuators and chambers (each represented by different colored air paths).

To be specific, as depicted in Figure 5, three units (Unit A, B, C) are interconnected end-to-end to form a ring oscillator, enabling sequential inflation and deflation of different actuators. Taking unit A as an example, it consists of a pair of soft actuators (A1, A2) moving synchronously in opposite directions. Additionally, two pairs of soft chambers with bistable membranes (A1', A2') are orthogonally positioned to facilitate bistable valve switching.

Furthermore, units A, B, and C share a common constant air supply, divided into inputs A, B, and C, respectively. However, their outputs lead to different destinations. For instance, the outputs of unit A, denoted as output A and A' in Figure- 5, is connected to the soft chamber switch of unit B as a signal. Specifically, output A is linked to B1', and output A' is linked to B2', establishing a functional relationship between unit A and unit B. It's important to note that output A not only serves as an actuation signal for actuator A1 but also controls the switch of unit B. Similarly, unit B governs unit C, and the output of unit C is looped back to unit A, facilitating the continuous cycle of the entire system.

Figure 6 illustrates the entire oscillation cycle, which consists of six stages (with all parts named according to the same rules as in Figure 5). It commences with the deflation of all actuators and bistable chambers when there is no air supply. Upon initiating the air supply, compressed air reaches all three units within 1 second.

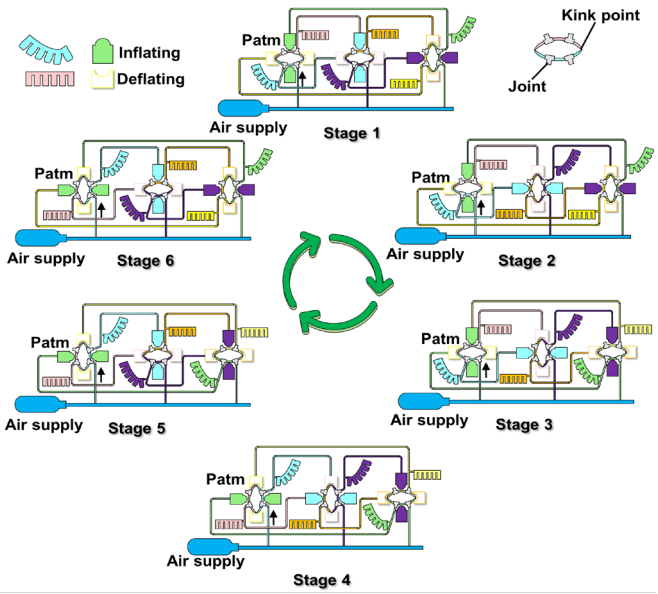

Figure 6. The whole cycle the ring oscillators based on our proposed bistable valve (all air paths are represented by different colors)

In Stage 1, actuators A1, B1, and C2 inflate, while actuators A2, B2, and C1 deflate. Stage 2 sees the inflation of chamber B1' and the deflation of chamber B2' through outputs A and A', resulting in the reversal of the bistable valve state in unit 2. Corresponding adjustments occur in the inflation and deflation channels, with actuator B2 inflating and actuator B1 deflating.

In Stage 3, the valve state of unit 3 undergoes a transformation, leading to an alteration that propagates throughout the interconnected system, resulting in a specific pattern of oscillation in the actuators. For example, actuators A1, B1, C1 will oscillate at a fixed phase offset, while A2, B2, C2 will generate synchronized opposite oscillations to those of actuators A1, B1, C1.

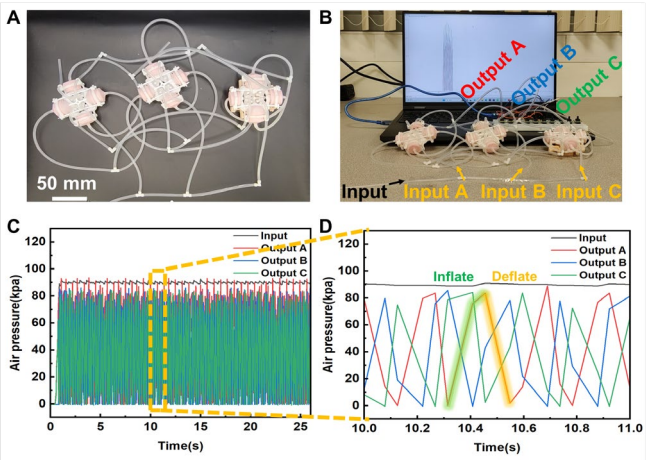

Figure 7. Electronics-free ring oscillator. A) Three units are connected end-to-end to form a soft ring oscillator, enabling sequential inflation and deflation of different chambers (each represented by different colored air paths). B) Real-time monitoring settings of outputs A-C. C) and D) Pressure plots at the three nodes of the oscillator when input pressurized is 90 KPa.

As shown in Figure 7A, we connected three valves in an end-to-end manner, and tested the air pressure time-lapse curves of outputs A, B, and C using an air pressure real-time monitoring module (As shown in Figure 7B). Figures 7C and 7D illustrate the variations in air pressure of outputs A, B, and C. The air pressure ranges between 0 and 90 KPa with a frequency of approximately 5 Hz when a 90 KPa air pressure is applied. Additionally, we observe the oscillation sequence of A-B-C due to the end-to-end connection of units A, B, and C.

VI. Materials and Methods

All molds and frameworks used in this work were fabricated using a desktop commercial Fused Deposition Modeling (FDM) 3D printer, specifically the Ender-3 V2 by CREALITY Inc. We opted for Polylactic Acid (PLA) filament due to its moderate strength and toughness. The printing settings were configured as follows: a printing temperature of 200°C, a build plate temperature of 60°C, a layer height of 0.12 mm, and an infill density of 30%.

For all elastomeric components in this study, we utilized commercially available Smooth-On: Smooth-Sil 940. We mixed Smooth-Sil 940 components 'A' and 'B' in a 10:1 weight ratio, manually stirred the mixture for 2 minutes, and subsequently degassed it for 3 minutes under vacuum. After pouring the degassed Smooth-Sil 940 mixture into the 3D-printed molds, we cured it at 55°C for 20 minutes to fabricate the components for all of the soft devices.

To connect and affix a commercial soft silicone tube (with an outer diameter of 3mm and an inner diameter of 2mm) to the elastomeric shell, we employed a liquid Smooth-Sil 940 mixture and cured it at 50°C for 5 minutes to create chambers with bistable membranes and soft pneumatic actuators. We also conducted tests to ensure their airtightness. The fabrication process for the soft fingers mirrors the aforementioned procedure. The final step involves assembling all the components and conducting sealing performance tests on all parts.

The real-time air pressure monitoring module is established based on the microcontroller (Arduino mega 2560) and pressure sensors(-100KPa~300KPa).

VII. Conclusion

In this study, we have conceptualized and developed a simple yet highly efficient electronics-free valve that excels in providing synchronous reverse outputs, storing valve status, and facilitating maintenance. Through both experimental observations and finite element method (FEM) analysis, our soft valve has demonstrated a bistable property.

Our valve exhibits the versatility to be operated both manually and pneumatically. For manual operation, we have showcased its integration into a soft gripper as a contact sensor. Our gripper, equipped with the bistable valve, showcases efficient grasping capabilities on human fingers, tape, and soft pneumatic artificial muscles.

Additionally, pneumatic operation is feasible for our valve by incorporating two pairs of soft chambers. We have also introduced a framework to enhance switch speed and prevent air leakage. With this design, our valve achieves self-oscillation, synchronous reverse outputs, and high frequency (easily reaching a frequency of 5 Hz with an 80

KPa air pressure, and a frequency of approximately 12 Hz was detected when 150 KPa of air pressure was applied).

Furthermore, we have demonstrated the feasibility of constructing a ring oscillator using three units, achieving sequential outputs with a moderate frequency (approximately 5 Hz detected with a 90 KPa air pressure).

Moreover, owing to its bistable structures, the valve's state remains unchanged even in the event of sudden air supply shutdowns, and its state can only be altered when air supply is reapplied. Additionally, the unenclosed design facilitates easy disassembly, replacement, and maintenance of parts.

In summary, we present a simple yet powerful pneumatic, bistable electronics-free valve. We believe it can serve as a platform for the development of untethered and autonomous electronics-free pneumatic soft robots, including soft walking robots (bipedal, quadrupedal, and multi-legged), swimming robots, and even flapping-wing flying robots.

ACKNOWLEDGMENTS

This work was supported by the NUS research scholarships and start-up grant RoboLife (Soft Robots with morphological adaptation and life-like abilities), DESTRO (Dextrous, strong yet soft robots), ITALY–SINGAPORE grant, MAE (Italy) and A*STAR (Singapore), Grant # R22I0IR124, and REBOT (Rethinking underwater robot manipulation), Ministry of Education, Singapore, Grant #T2EP50221-0028.

REFERENCES

[1] C. Laschi and M. Cianchetti, "Soft Robotics: New Perspectives for Robot Bodyware and Control," Front Bioeng Biotechnol, vol. 2, p. 3, 2014, doi: 10.3389/fbioe.2014.00003.

[2] S. Kim, C. Laschi, and B. Trimmer, "Soft robotics: a bioinspired evolution in robotics," Trends Biotechnol, vol. 31, no. 5, pp. 287-94, May 2013, doi: 10.1016/j.tibtech.2013.03.002.

[3] L. Kan, Z. Wu, B. Song, B. Su, and Y. Shi, "Bioinspired Centimeter-scale Sensor Free Obstacle-passing Robots with a Wireless Control System," Journal of Bionic Engineering, vol. 19, no. 4, pp. 953-964, 2022, doi: 10.1007/s42235-022-00186-0.

[4] W. Li, D. Hu, and L. Yang, "Actuation Mechanisms and Applications for Soft Robots: A Comprehensive Review," Applied Sciences, vol. 13, no. 16, 2023, doi: 10.3390/app13169255.

[5] P. Wang, Z. Tang, W. Xin, Z. Xie, S. Guo, and C. Laschi, "Design and Experimental Characterization of a Push-Pull Flexible Rod-Driven Soft-Bodied Robot," IEEE Robotics and Automation Letters, vol. 7, no. 4, pp. 8933-8940, 2022, doi: 10.1109/lra.2022.3189435.

[6] V. Cacucciolo, J. Shintake, Y. Kuwajima, S. Maeda, D. Floreano, and H. Shea, "Stretchable pumps for soft machines," *Nature,* vol. 572, no. 7770, pp. 516-519, Aug 2019, doi: 10.1038/s41586-019-1479-6.

[7] L. Kan, F. Lei, B. Song, B. Su, and Y. Shi, "Flexible electromagnetic capturer with a rapid ejection feature inspired by a biological ballistic tongue," Bioinspir Biomim, vol. 15, no. 6, Sep 11 2020, doi: 10.1088/1748-3190/aba444.

[8] M. Wehner *et al.*, "An integrated design and fabrication strategy for entirely soft, autonomous robots," *Nature,* vol. 536, no. 7617, pp. 451-5, Aug 25 2016, doi: 10.1038/nature19100.

[9] Z. Tang et al., "Meta-Learning-Based Optimal Control for Soft Robotic Manipulators to Interact with Unknown Environments," presented at the 2023 IEEE International Conference on Robotics and Automation (ICRA), 2023.

[10] M. S. Nazeer, C. Laschi, and E. Falotico, "Soft DAgger: Sample-Efficient Imitation Learning for Control of Soft Robots," Sensors, vol. 23, no. 19, 2023, doi: 10.3390/s23198278.

[11] T. George Thuruthel, Y. Ansari, E. Falotico, and C. Laschi, "Control Strategies for Soft Robotic Manipulators: A Survey," Soft Robot, vol. 5, no. 2, pp. 149-163, Apr 2018, doi: 10.1089/soro.2017.0007.

[12] L. C. van Laake, J. de Vries, S. Malek Kani, and J. T. B. Overvelde, "A fluidic relaxation oscillator for reprogrammable sequential actuation in soft robots," Matter, vol. 5, no. 9, pp. 2898-2917, 2022, doi: 10.1016/j.matt.2022.06.002.

[13] X. Zhang, A. E. Oseyemi, S. Yu, and Q. Gu, "Fully soft valve for autonomous pressure control," presented at the 2021 3rd International Symposium on Robotics & Intelligent Manufacturing Technology (ISRIMT), 2021.

[14] D. J. Preston et al., "Digital logic for soft devices," Proc Natl Acad Sci U S A, vol. 116, no. 16, pp. 7750-7759, Apr 16 2019, doi: 10.1073/pnas.1820672116.

[15] P. Rothemund et al., "A soft, bistable valve for autonomous control of soft actuators," Sci Robot, vol. 3, no. 16, Mar 21 2018, doi: 10.1126/scirobotics.aar7986.

[16] D. J. Preston et al., "A soft ring oscillator," Sci Robot, vol. 4, no. 31, Jun 26 2019, doi: 10.1126/scirobotics.aaw5496.

[17] S. V. Kendre et al., "The Soft Compiler: A Web-Based Tool for the Design of Modular Pneumatic Circuits for Soft Robots," IEEE Robotics and Automation Letters, vol. 7, no. 3, pp. 6060-6066, 2022, doi: 10.1109/lra.2022.3159858.

[18] M. Garrad, I. Feeney, A. T. Conn, J. Rossiter, M. P. Nemitz, and H. Hauser, "An all soft, electro-pneumatic controller for soft robots," presented at the 2021 IEEE 4th International Conference on Soft Robotics (RoboSoft), 2021.

[19] X. Zhang, A. E. Oseyemi, S. Yu, and Q. Gu, "Fully soft valve for autonomous pressure control," presented at the 2021 3rd International Symposium on Robotics & Intelligent Manufacturing Technology (ISRIMT), 2021.

[20] W. K. Lee et al., "A buckling-sheet ring oscillator for electronics-free, multimodal locomotion," Sci Robot, vol. 7, no. 63, p. eabg5812, Feb 9 2022, doi: 10.1126/scirobotics.abg5812.

[21] D. Drotman, S. Jadhav, D. Sharp, C. Chan, and M. T. Tolley, "Electronics-free pneumatic circuits for controlling soft-legged robots," Sci Robot, vol. 6, no. 51, Feb 17 2021, doi: 10.1126/scirobotics.aay2627.

[22] K. Luo, P. Rothemund, G. M. Whitesides, and Z. Suo, "Soft kink valves," Journal of the Mechanics and Physics of Solids, vol. 131, pp. 230-239, 2019, doi: 10.1016/j.jmps.2019.07.008.

[23] J. A. Tracz et al., "Tube-Balloon Logic for the Exploration of Fluidic Control Elements," IEEE Robotics and Automation Letters, vol. 7, no. 2, pp. 5483-5488, 2022, doi: 10.1109/lra.2022.3156174.

[24] Y. Zhai et al., "Desktop fabrication of monolithic soft robotic devices with embedded fluidic control circuits," Sci Robot, vol. 8, no. 79, p. eadg3792, Jun 21 2023, doi: 10.1126/scirobotics.adg3792.

[25] S. Conrad et al., "3D-printed digital pneumatic logic for the control of soft robotic actuators," Science Robotics, vol. 9, no. 86, p. eadh4060, 2024.

[26] S. V. Kendre et al., "The Soft Compiler: A Web-Based Tool for the Design of Modular Pneumatic Circuits for Soft Robots," IEEE Robotics and Automation Letters, vol. 7, no. 3, pp. 6060-6066, 2022, doi: 10.1109/lra.2022.3159858.

[27] K. Xu and N. O. Perez-Arancibia, "Electronics-Free Logic Circuits for Localized Feedback Control of Multi-Actuator Soft Robots," IEEE Robotics and Automation Letters, vol. 5, no. 3, pp. 3990-3997, 2020, doi: 10.1109/lra.2020.2982866.

[28] C. J. Decker et al., "Programmable soft valves for digital and analog control," Proc Natl Acad Sci U S A, vol. 119, no. 40, p. e2205922119, Oct 4 2022, doi: 10.1073/pnas.2205922119.

[29] J. K. Choe, J. Kim, H. Song, J. Bae, and J. Kim, "A soft, self-sensing tensile valve for perceptive soft robots," Nat Commun, vol. 14, no. 1, p. 3942, Jul 4 2023, doi: 10.1038/s41467-023-39691-z.